Title
NON-PERIPHERAL COLLISIONS OF HEAVY IONS IN NUCLEAR EMULSION

Author
Heckman, H.H.

Publication Date
1977-07-01

Proceedings of the Meeting on Heavy Ion Collisions, Falls Creek Falls State Park, TN, June 13 - 17, 1977

LBL-6562 c-1

NON-PERIPHERAL COLLISIONS OF HEAVY IONS IN NUCLEAR EMULSION

H. H. Heckman, H. J. Crawford, D. E. Greiner, P. J. Lindstrom, and L. W. Wilson

July 1977

Prepared for the U. S. Energy Research and Development Administration under Contract W-7405-ENG-48

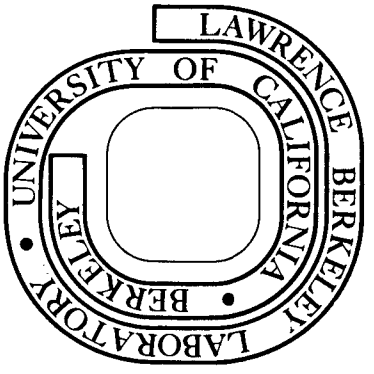

LBL-6562 c-1

DISCLAIMER

LBL-6562

NON-PERIPHERAL COLLISIONS OF HEAVY IONS IN NUCLEAR EMULSION

H.H. Heckman, H.J. Crawford, D.E. Greiner, P.J. Lindstrom, and L.W. Wilson
Lawrence Berkeley Laboratory and Space Sciences Laboratory
University of California, Berkeley, California 94720 U.S.A.

Introduction: Because of the large range of ionization and multiplicities of fragments that are produced in collisions between heavy ions, electron-sensitive nuclear track emulsions are particularly suited for studies of heavy ion interactions owing to their high-spatial resolution and unrestricted sensitivity to rates of energy loss. We are presently carrying out an experimental study using the emulsion technique to examine the angular and momentum distributions of fragments emitted from non-peripheral collisions between emulsion nuclei (AgBr) and heavy-ion projectiles ^{4}He, ^{16}O, and ^{40}Ar in the range of energies 0.2 to 2.1 GeV/A. The beams and their specific energies used for the experiment are:

Beam	Energy(GeV/A)
^{4}He	2.1, 1.05
^{16}O	2.1, 0.20
^{40}Ar	1.8

Selection Criteria: The selection criterion we have adopted for a non-peripheral collision is that the interaction exhibits an absence of projectile fragmentation, i.e., an interaction where no beam-velocity fragments ($Z_F \geq 1$ from ^{4}He interactions, $Z_F \geq 2$ from ^{16}O and ^{40}Ar interactions) are produced within 5° (when E_{beam} = 1.05 and 2.1 GeV/A) or 10° (when E_{beam} = 0.20 GeV/A) of the incident beam direction. Interactions selected under this criterion are

deemed to be "central" collisions between the projectile and target nuclei, qualitatively characterized by impact parameters that are in the range $0 \leqslant b \lesssim |R_T - R_p|$.

Scanning and Measuring: Both along-the-track and volume scanning techniques were used to locate events. All track-coordinate measurements were made under oil-immersion objectives, 1000x total magnification, using three-coordinate digitally-encoded microscopes.

Measurements: For those heavy-ion interactions that satisfied the selection criterion, the following measurements of angle and track range were carried out for each beam nucleus:

1) The production angles were measured for all secondary fragments having a restricted grain density $g \geqslant 2\ g_{min}$, after correcting for the dip angle. (A Z=1 particle with $g \geqslant 2\ g_{min}$ has an energy $E \leqslant 250$ MeV/A.)
2) Track ranges and angles were measured for a subset of fragments with ranges $\leqslant 4$ mm, with no minimum range cutoff except that due to obscuration of short tracks at the point of interaction. (A 4 mm range in emulsion corresponds to proton and ^{4}He energies equal to 31 MeV/A.)
3) Each fragment measured under (1) was classified as to whether its potential range was less or greater than 4 mm. This visual estimate of potential range was made by the scanner-measurer by observing the grain density ($g \geqslant 10\ g_{min}$ for protons) and multiple scattering of the track in the pellicle containing the event.

In order to identify data measured under the above procedures, we shall use the notation "$E_p <$" to signify data whose energy limits are made either by measurements of grain density (1), or by estimated range (3). Data identified by $R \leqslant 4$ mm (2), for which $\in$ = E/A = 31 MeV/A for protons and ^{4}He, will signify that the data are based on actual range measurements.

Analytic Procedure: Owing to the high excitation energies and the large average number of particles that partake in non-peripheral (central) collisions of the type selected for this investigation, we make the practical assumption that the system we are considering is large enough and the mutual interactions are strong enough so that it can be described statistically, based on the hypothesis of equal *a priori* probabilites in phase space. Such a statistical distribution is the Maxwell-Boltzmann distribution. This distribution, expressed in a covariant, non-relativistic form, in terms of the velocity β of the emitted fragments appropriate for the range of velocities we consider in this experiment is as follows:

$$d^2N/d\beta d\mu \propto \beta^2 e^{-(\beta^2 - 2\beta\bar{\beta}_{||}\mu)/\bar{\beta}_o^2} \qquad (1)$$

where $\bar{\beta}_{||}$ is the longitudinal velocity of the particle-emitting system, $\mu = \cos\theta$, where θ is the laboratory angle between the momenta of the fragment of mass M and the incident projectile, and $\bar{\beta}_o = \sqrt{2\tau/M_n}$ is the characteristic spectral velocity of Maxwell-Boltzmann distribution. The effective "temperature" of the system is τ(MeV/A), for a fragment of mass $M = AM_n$.

We now express Eq. 1 in terms of range R and μ, the two quantities measured in this experiment. In general, the velocity $\beta(\approx P/M)$ of a particle

with mass M and charge z, having a residual range R is given by the relation

$$\beta = f(Rz^2/M). \tag{2}$$

To good approximation, the R-β relation for nuclear emulsion is given by the power-law expression

$$\beta = k(Rz^2/m)^n \tag{3}$$

where k = 0.174, n = 0.29, R is in mm, and z and m are the atomic mass number and mass of the fragment, respectively, the latter being in units of the proton mass, i.e., $m = M/M_p$. In terms of range R and $\mu = \cos\theta$, the Maxwell-Boltzmann distribution (Eq. 1) becomes

$$d^2N/dRd\mu \propto (z^2/m)^{3n} R^{3n-1} e^{-(k^2R^{2n} - 2kR^n\beta_{||}\mu)/\beta_o^2} \tag{4}$$

where

$$\beta_{||} = \bar{\beta}_{||}(m/z^2)^n \text{ and } \beta_o = \bar{\beta}_o(m/z^2)^n. \tag{5a}$$

It follows that the parameter we shall denote as

$$\chi_o = \beta_{||}/\beta_o = \bar{\beta}_{||}/\bar{\beta}_o, \tag{5b}$$

which is the ratio of the longitudinal velocity of the center of mass $\beta_{||}$ to the characteristic spectral velocity β_o of the fragmenting system, is common to both the velocity and range spectra, and is independent of (m,z).

Thus, the longitudinal velocity $\beta_{||}$ and spectral velocity β_o that characterize the range spectrum of unidentified fragments (Eq. 4) are related to the corresponding quantities for the velocity spectrum (Eq. 1) for any fragment (m,z) by the quantity $(m/z^2)^n$, where n is the range-velocity index. In this experiment, the parameters $\beta_{||}$ and β_o are determined from the range and angle data using Eq. 4, assuming $m/z^2 = 1$, for which $\bar{\beta}_o = \beta_o$ and $\bar{\beta}_{||} = \beta_{||}$. By fitting the measured range and angle data to evaluate $\beta_{||}$ and β_o we are effectively testing how well such data can be described given the following assumptions:

i) the observed range and angle distributions are interpretable in terms of a single Maxwellian-range (velocity) distribution,

ii) the isotopic distribution of fragments is dominated by one species, i.e., protons, thereby minimizing any significant difficulties in defining β_o in the Maxwell distribution (Eq. 1), and

iii) to the extent that (ii) is satisfied, the $\beta_{||}$ and β_o parameters that characterize the range and angular distributions are the same as those that describe the velocity distribution for nucleons.

Experimental Results:

A. *Prong number distributions.* Figure 1 presents the distributions of prong number per event, N_p, for the interactions of each heavy ion beam (^{4}He and ^{16}O at 2.1 GeV/A, ^{40}Ar at 1.8 GeV/A) selected under the criteria previously described. The prong distributions for the lower energy ^{4}He and ^{16}O beams are similar to those shown. The distributions pertain to charged prongs having restricted grain densities $g \geqslant 2\ g_{min}$, i.e., equivalent to proton energies $\leqslant 250$ MeV, emitted from events selected only when the projectile was fully occulted by the target nucleus. If we first consider the multiplicity

distributions of prongs arising from ^{40}Ar and ^{16}O collisions, we note that each distribution shows a single maximum and is approximately symmetric about its mean-prong number. In contrast, the N_p-distribution for ^4He projectiles shows two maxima, one in the region of N_p = 6 to 8, and the other at $N_p \approx 19$. We attribute the low-prong-number peak to collisions between the ^4He projectile and CNO (light) nuclei, and the high-prong-number peak to collisions with AgBr (heavy) nuclei because ^4He can be occulted in CNO as well as in AgBr collisions. The absence of a CNO peak in the ^{16}O and ^{40}Ar prong distributions indicates that the non-occultation of these projectiles by the light CNO target nuclei invariably shows visual evidence for projectile fragmentation. Thus, by eliminating prong numbers $N_p \leqslant 9$ from the ^4He data, we limit the interactions of high energy ^4He, ^{16}O, and ^{40}Ar nuclei to near-central collisions with Ag and Br with little, if any, contribution to the data from collisions with lighter emulsion nuclei.

B. *Range and angular distributions:* $R \leqslant 4$ *mm.* Measurements of the ranges and angular distribution of the fragments with $R \leqslant 4$ mm permit us to determine the velocity-parameters $\beta_{||}$ and β_o, and therefore χ_o, by least-squares fits of these data to Eq. 4. These parameters are tabulated in Table I. One of the features of these data is the near independence of the range and angular distributions for fragments with $R \leqslant 4$ mm, with respect to the mass of the projectile at beam energy 2.1 (1.8) GeV/A, as indicated by the approximate constancy of each of the fitted parameters. The longitudinal velocities of the particle-emitting systems, $\beta_{||}$, increase with decreasing beam energy, whereas the spectral velocities appear to be equal to within 10%, irrespective of the mass and energy of the projectile. The values of $\beta_{||}$ are in close agreement

with those measured for low-energy fragment-emitting systems produced in a variety of nucleus-nucleus and proton-nucleus collisions over a broad range of energies.[1,2] The temperature τ implied by the velocities $\beta_o = \sqrt{2\tau_n/M_n}$ are typically 6-7 MeV/A, characteristic of the binding energies of nuclei, and also compatible with the temperatures associated with projectile fragmentation.[3,4]

In Fig. 2 we present an example of the range-angle data obtained at beam energies 2.1 (1.8) GeV/A in terms of the rapidity variable $y \approx \beta_L$ ($y = \tanh^{-1}\beta_L$), where β_L is the longitudinal component of the quantity $\vec{\beta} = k(Rz^2/m)^n$, assuming $z^2/m = 1$. The mean value $\langle y \rangle = \beta_{||}$ is indicated for each distribution, as is the standard deviation $\sigma = \beta_o/\sqrt{2} = \sqrt{\tau/M_n}$. The average standard deviation of the three rapidity distributions is $\langle \sigma \rangle = 0.082 \pm 0.001$, which corresponds to a longitudinal momentum $P_L = 77$ MeV/c per nucleon.

C. *Angular distributions.* Examples of the angular distributions observed for fragments with energies $E_p < 31$ MeV and $E_p < 250$ MeV obtained with 2.1 (1.8)-GeV/A beam projectiles are shown in Figs. 3 and 4, respectively. The distributions are presented as functions of both θ and $\cos\theta$. Drawn through the data are curves derived from the fitted Maxwell-Boltzmann distributions. Because the angular distributions of the low energy fragments $E_p \leqslant 31$ MeV (Fig. 3) were taken without knowledge of particle ranges, subject only to the condition that $E_p < 31$ MeV, we found that the minimum χ^2-fits did not yield unique values for $\beta_{||}$ and β_o, but rather gave values of $\beta_{||}$ and β_o that were linearly coupled. Thus, we chose to fix β_o at the value determined previously from the range-angle data and evaluate $\beta_{||}$. The values thus obtained are indicated in Fig. 3 , along with the appropriate β_o's taken from Table I.

When the angular distribution of fragments is measured without regard to fragment velocity, $dN/d\mu$ (Eq. 1) becomes a function of $\chi_o \equiv \beta_{||}/\beta_o$ only. We have fitted the measured angular distribution for fragments with $E_p < 250$ MeV to this asymptotic form of the angular distribution to obtain one-parameter fits to the data (Fig. 4).

Figs. 5 and 6 show the angular distributions $dN/d\cos\theta$ vs. $\cos\theta$ for $E_p <$ 31 MeV and $E_p < 250$ MeV, respectively, for the lowest beam energy, ^{16}O at 0.20 GeV/A. The notable difference between the ^{16}O-produced fragments at 2.1 and 0.2 GeV/A is the significant increase in the relative production of fragments $E_p < 31$ and $E_p < 250$ MeV, in the forward hemisphere as the beam energy decreases. The shift of the angular distribution of the low energy fragments $E_p < 31$ MeV to smaller forward angles is due to an increase in $\beta_{||}$, 0.017 to 0.039, while the spectral velocity (temperature), based on the results of the $R \leq 4$ mm data (Table I), remains essentially constant, i.e., 0.106-0.115 (5.3-6.2 MeV/A). For energies $E_p < 250$ MeV, the distribution of fragments produced by 0.20 GeV/A ^{16}O is increasingly peaked forward, indicated by the fact that $\chi_o \equiv \beta_{||}/\beta_o$ increases from 0.26 to 0.62 as the beam energy decreases from 2.1 to 0.20 GeV/A.

The beam-energy dependence of the angular distribution data for ^4He and ^{16}O projectiles are summarized in Tables II and III. Here we give the values of the parameter $\chi_o = \beta_{||}/\beta_o$ obtained by fitting the angular distributions in the backward, forward and combined hemispheres, for $E_p < 31$ and $E_p < 250$ MeV, respectively.

Salient features of the angular distributions are:

For $E_p < 31$ MeV,

1) The values of χ_o for the combined hemispheres, $-1 \leq \mu \leq 1$, increase with decreasing E_{beam}.
2) The change in $\chi_o(-1 \leq \mu \leq 1)$ is primarily due to the increase in χ_o for the forward hemisphere, i.e., the angular distribution becomes more anisotropic.
3) At 2.1 GeV/A beam energy, the fragments are consistent with isotropy in the laboratory, $\chi_o(0 \leq \mu \leq 1) \approx 0$. (This is illustrated in Fig. 3.)
4) The angular distribution in the backward hemisphere is essentially invariant with respect to beam and energy. Note the near equality of the values of $\chi_o(-1 \leq \mu \leq 0)$ for the pairs of ^{4}He and ^{16}O data, Table II.

For $E_p < 250$ MeV,

1) The angular distributions are more anisotropic than those at $E_p < 31$ MeV.
2) The shape of the angular distributions in backward hemisphere remains invariant with respect to beam and energy. The values $\chi_o(-1 \leq \mu \leq 0)$ for ^{4}He and ^{16}O are, pairwise, the same.
3) The values of $\chi_o(0 \leq \mu \leq 1)$ increase with decreasing beam energy. At 2.1 GeV/A, fragment production continues to be more isotropic in the forward, relative to the backward, hemisphere (Fig. 4).

Some general conclusions of the experiment are (not all of which are obvious from this preview of the data):

1) There is no unique particle-emitting system, characterized by a center-of-mass velocity $\beta_{||}$ and spectral velocity $\beta_o = \sqrt{2\tau/M_n}$, that accounts for the spectra of fragment ranges (momenta) and angles.
2) The $dN/d\theta$ distributions are broad, Maxwellian-like, with maxima that

shift toward smaller angles as the fragment energy increases, and as beam energy decreases.

3) No statistically significant structure, attributable to well-defined collective phenomena, is observed in the range or angular distributions.

4) By invoking the results of Ref. 5, there is no evidence that the angular distribution for low-energy fragments depends on the impact parameters of the collision between heavy ions at E_{beam} = 2.1 GeV/A.

5) At beam energy 2.1 (1.8) GeV/A, the number of fragments per event that are emitted in the backward hemisphere is insensitive to the projectile mass, e.g. 6.8, 6.7, and 7.1 for ^{4}He, ^{16}O, and ^{40}Ar, respectively.

Acknowledgements. We thank Margret Banks, Hester Yee, and Robert Turner for their assistance in scanning the nuclear emulsions. We also appreciate the guidance and advice given us by Dr. T.F. Hoang in the analysis and interpretation of the data. This work was carried out under the auspices of U.S. Energy Research and Development Administration, Contract W-7405-ENG-48 and the National Aeronautics and Space Administration, Grant NGR 05-003-513.

REFERENCES

1. E.K. Hyde, G.W. Butler, and A.M. Poskanzer, Phys. Rev. C 4, 1759 (1971).

2. H.H. Heckman, LBL Report 6561 (to be published).

3. D.E. Greiner, P.J. Lindstrom, H.H. Heckman, Bruce Cork, and F.S. Bieser, Phys. Rev. Lett. 35, 152 (1975).

4. A.S. Goldhaber, Phys. Lett. 53B, 306 (1974).

5. G.M. Chernov, K.G. Gulamov, U.G. Gulyamov, S.K. Nasyrov, and L.N. Svechnikova, Nucl. Phys. A280, 478 (1977).

TABLE I. Fitted parameters $\beta_{||}$, β_o, and $\chi_o \equiv \beta_{||}/\beta_o$ obtained from the range and angular distributions of fragments, $R \leq 4$ mm ($\in$ = 31 MeV/A).

E_{beam} (GeV/A)		^{4}He	^{16}O	^{40}Ar
2.1 (1.8)	$\beta_{||}$	0.016 ± 0.004	0.015 ± 0.002	0.012 ± 0.002
	β_o	0.117 ± 0.002	0.115 ± 0.002	0.117 ± 0.002
	χ_o	0.14 ± 0.04	0.13 ± 0.02	0.10 ± 0.02
1.05	$\beta_{||}$	0.021 ± 0.001		
	β_o	0.116 ± 0.002		
	χ_o	0.18 ± 0.01		
0.20	$\beta_{||}$		0.38 ± 0.003	
	β_o		0.106 ± 0.002	
	χ_o		0.36 ± 0.03	

TABLE II. Parameter $\chi_o \equiv \beta_{\parallel}/\beta_o$ for the Maxwellian distribution (Eq. 1) fitted to the angular distributions of fragments with $E_p < 31$ MeV. The values of β_o are given for the backward, forward, and combined hemispheres.

E_{beam}	Beam	$-1 \leqslant \mu \leqslant 0$	$0 \leqslant \mu \leqslant 1$	$-1 \leqslant \mu \leqslant 1$
0.20	^{16}O	0.33 ± 0.10	0.35 ± 0.05	0.37 ± 0.02
1.05	^{4}He	0.22 ± 0.07	0.20 ± 0.05	0.22 ± 0.06
2.1	^{16}O	0.31 ± 0.10	0.07 ± 0.07	0.15 ± 0.04
2.1	^{4}He	0.25 ± 0.07	0.05 ± 0.10	0.16 ± 0.02

TABLE III. Parameter χ_o for the Maxwellian distribution fitted to the observed angular distribution of fragments with $g > 2\ g_{min}$ ($E_p > 250$ MeV). The values of χ_o are given for the backward, forward, and combined hemispheres.

E_{beam}	Beam	$-1 \leqslant \mu \leqslant 0$	$0 \leqslant \mu \leqslant 1$	$-1 \leqslant \mu \leqslant 1$
0.20	^{16}O	0.41 ± 0.08	0.70 ± 0.04	0.62 ± 0.02
1.05	^{4}He	0.31 ± 0.09	0.34 ± 0.04	0.34 ± 0.02
2.1	^{16}O	0.37 ± 0.09	0.18 ± 0.03	0.26 ± 0.02
2.1	^{4}He	0.31 ± 0.08	0.24 ± 0.04	0.28 ± 0.03

FIGURE CAPTIONS

Fig. 1 Distribution of number of prongs (fragments) per event emitted from non-peripheral collisions with restricted grain densities $g > 2\ g_{min}$, corresponding to proton energies $E_p < 250$ MeV. Beam energies are 2.1 GeV/A for ^{4}He and ^{16}O, and 1.8 GeV/A for ^{40}Ar. The mean number of prongs/event, $\langle n \rangle$, are indicated. The CNO peak ($N_f \sim$ 6-8) is not included in the value of $\langle n \rangle$ for ^{4}He.

Fig. 2 Rapidity distributions $y = \beta_L$ of fragments with ranges $R \leq 4$ mm, assuming $m/z^2 = 1$. Cut-off values of $\beta_L = 0.26$ are indicated by the arrows on the abscissa. Values of $\beta_{\|}$ and $\beta_o = \sqrt{2}\sigma$ are given in Table I, $E_{beams} = 2.1\ (1.8)$ GeV/A.

Fig. 3 Angular distributions for fragments, $E_p < 31$ MeV. Solid curves are fits of the data to Eq. 1, $-1 \leq \cos\theta \leq 1$, using the parameters indicated. The dashed and dotted curves are fits to the data, for the backward and forward hemispheres, respectively.

Fig. 4 Angular distributions for fragments with $g < 2\ g_{min}$, $E_p < 250$ MeV. See caption Fig. 3 for identification of the plotted curves.

Fig. 5 Angular distribution $dN/d\cos\theta$ vs. $\cos\theta$ for fragments, $E_p < 31$ MeV. Projectile nucleus is ^{16}O at 0.2 GeV/A. The parameters of the fitted curve are $\beta_{\|} = 0.039$ and $\beta_o = 0.106$.

Fig. 6 Angular distribution $dN/d\cos\theta$ vs. $\cos\theta$ for fragments with $g \geq 2\ g_{min}$

($E_p < 250$ MeV). Projectile nucleus is ^{16}O at 0.2 GeV/A. The parameter for the fitted curve is $\chi_o = 0.62$. The data point at $\cos\theta = 0.9$ was not included in the fit, owing to a background of Z=1 fragments of the projectile not excluded by our selection criteria.

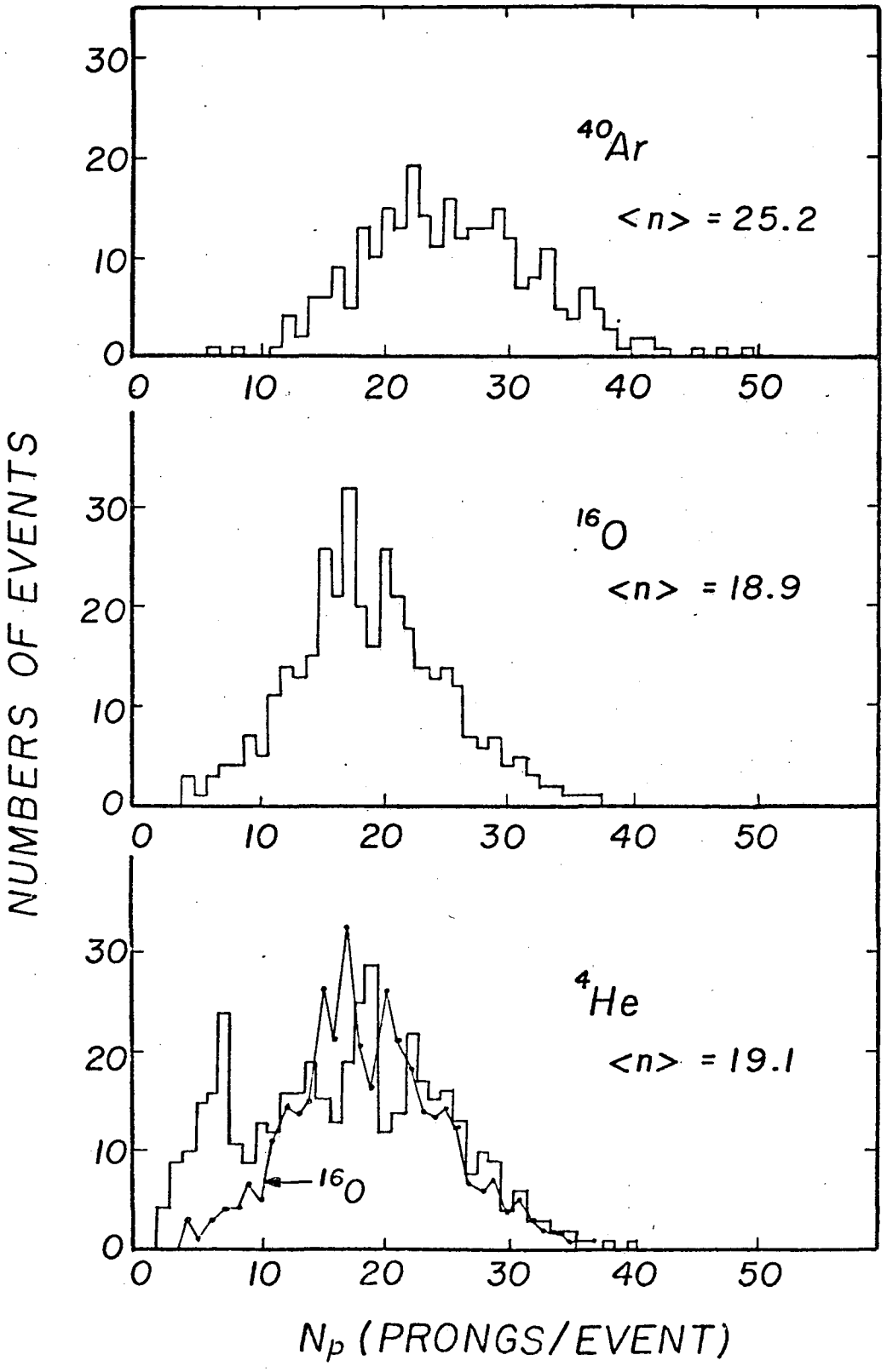
NUMBERS OF EVENTS
^{40}Ar
<n> = 25.2
^{16}O
<n> = 18.9
^{4}He
<n> = 19.1
^{16}O
0
10
20
30
40
50
N_p (PRONGS/EVENT)

FIGURE 1

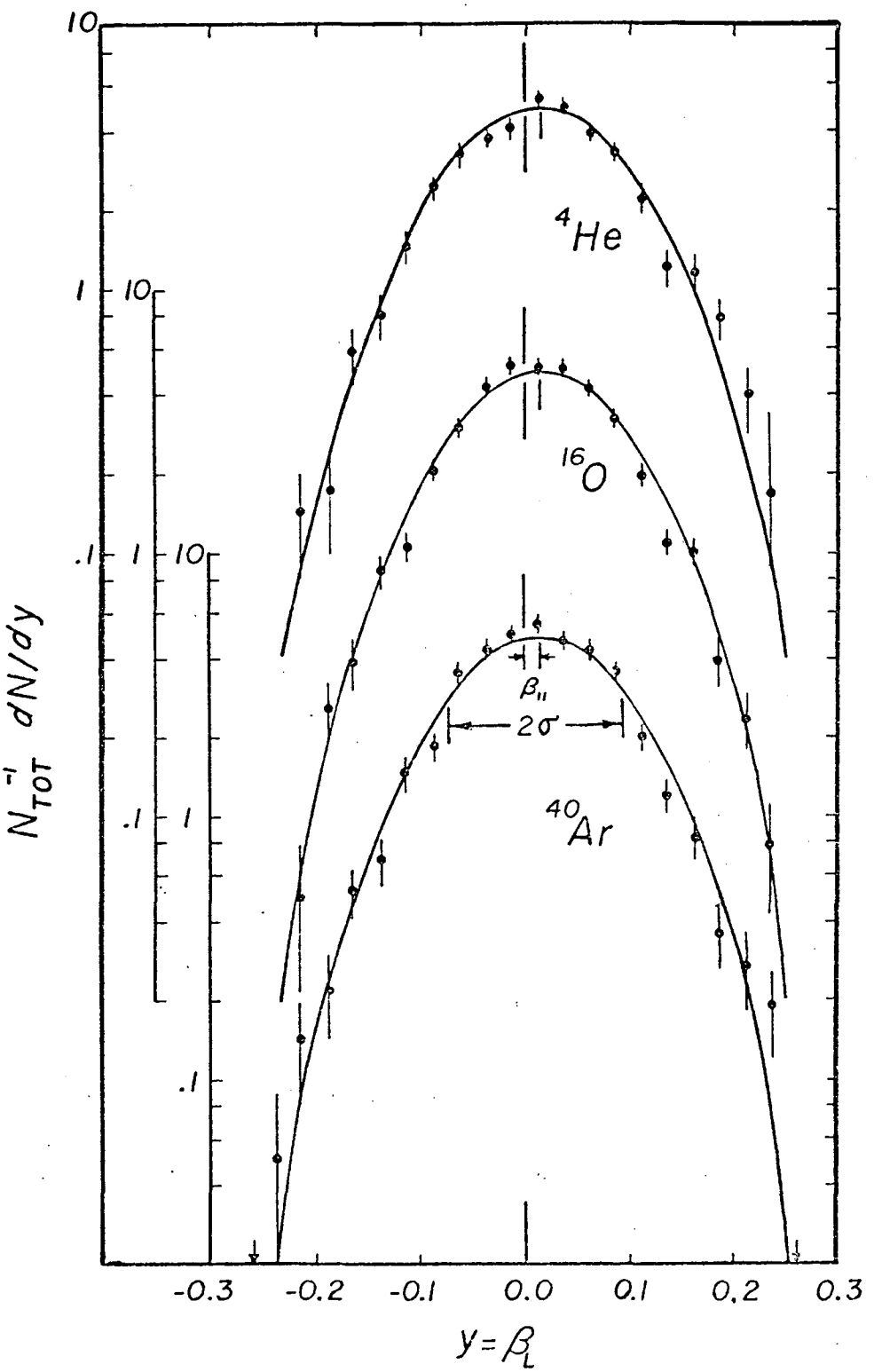
10
1
10
.1
1
10
.1
1
.1
^4He
^{16}O
^{40}Ar
β_{11}
2σ
$N_{TOT}^{-1}\ dN/dy$
-0.3
-0.2
-0.1
0.0
0.1
0.2
0.3
$y=\beta_L$

FIGURE 2

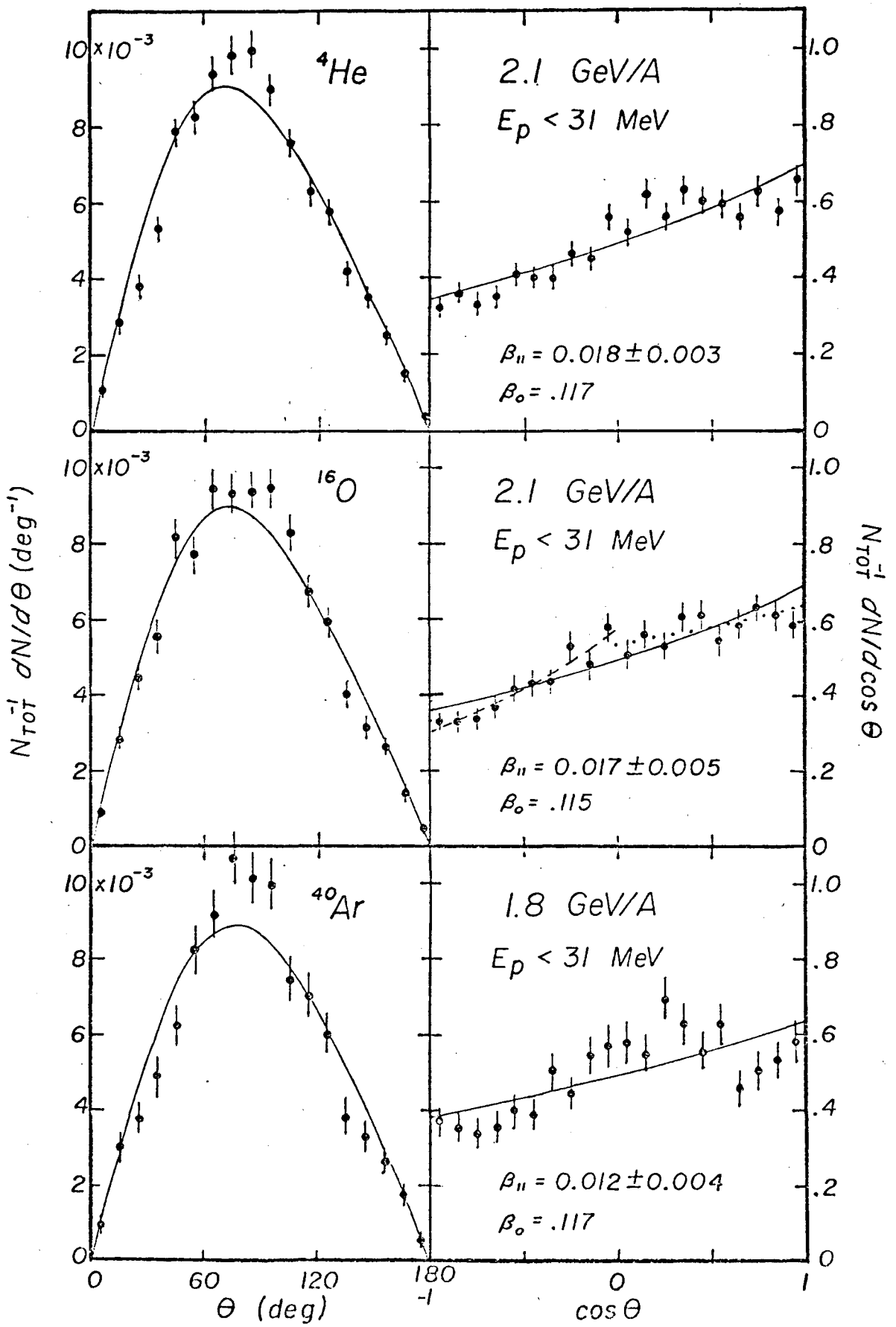

FIGURE 3

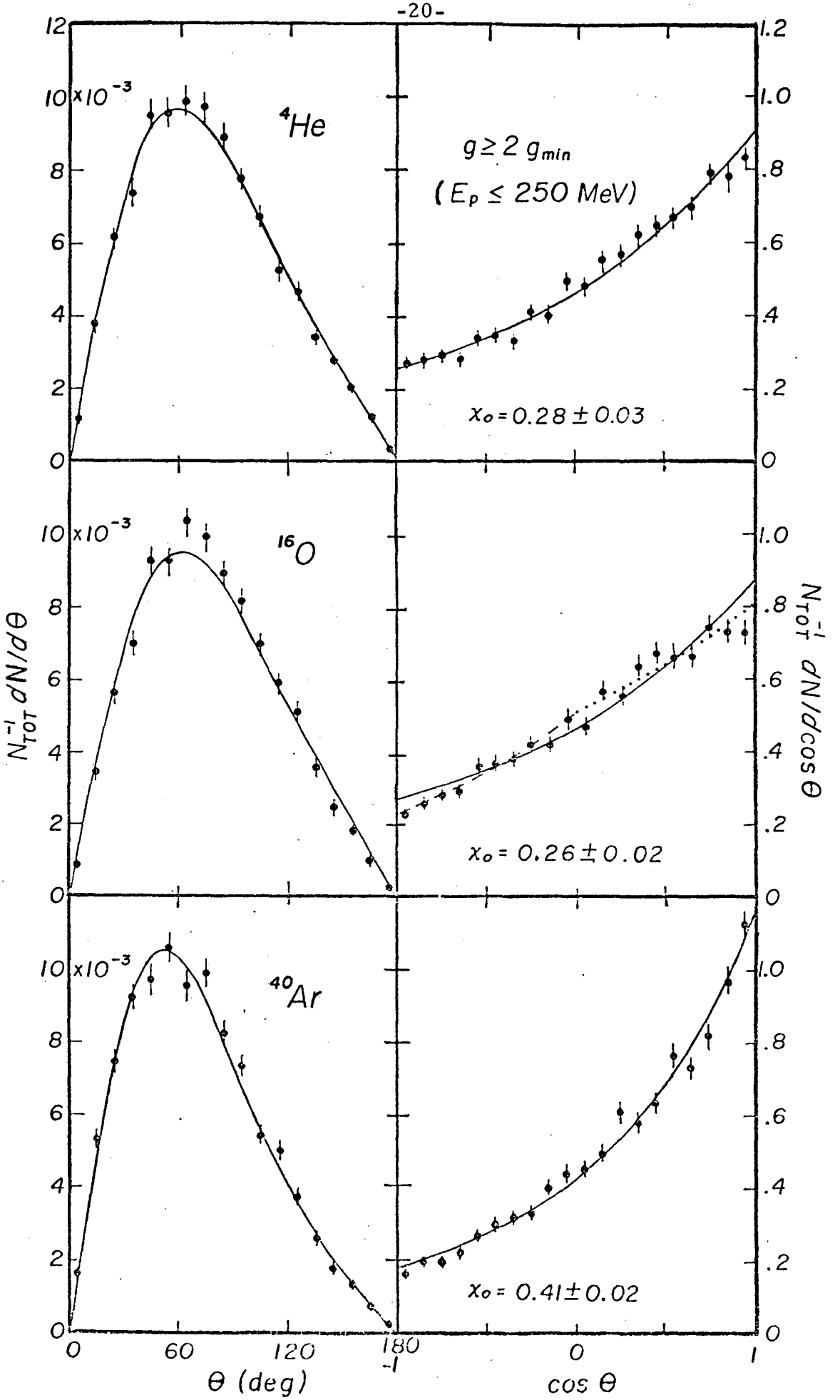
^4He
$g \geq 2\, g_{min}$
$(E_p \leq 250\ MeV)$
$x_o = 0.28 \pm 0.03$
^{16}O
$x_o = 0.26 \pm 0.02$
^{40}Ar
$x_o = 0.41 \pm 0.02$
$\times 10^{-3}$
$N_{TOT}^{-1}\, dN/d\theta$
$N_{TOT}^{-1}\, dN/d\cos\theta$
θ (deg)
$\cos\theta$

FIGURE 4

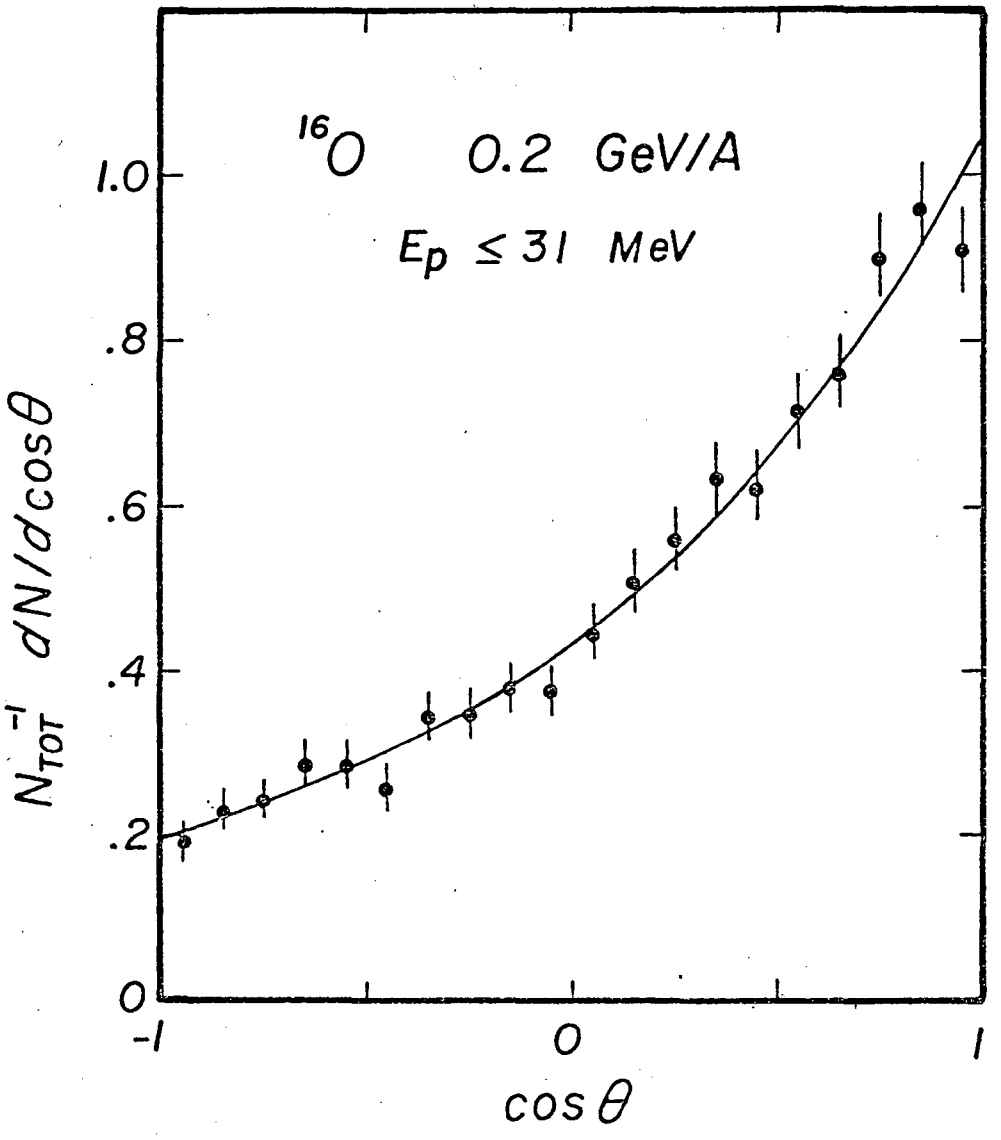
^{16}O 0.2 GeV/A
$E_p \leq 31$ MeV
1.0
.8
.6
.4
.2
0
-1
0
1
$N_{TOT}^{-1}\ dN/d\cos\theta$
$\cos\theta$

FIGURE 5

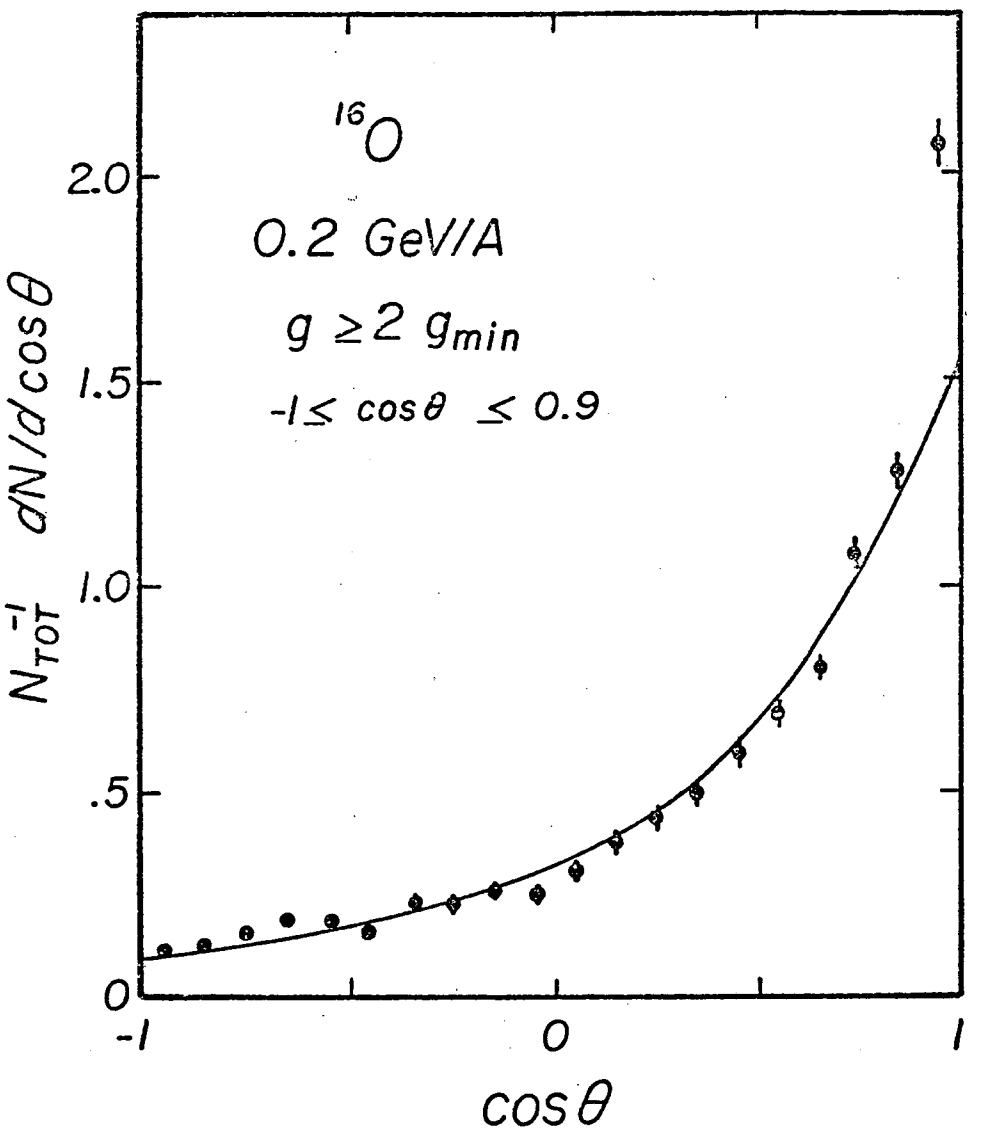
^{16}O
0.2 GeV/A
$g \geq 2\, g_{min}$
$-1 \leq \cos\theta \leq 0.9$
$N_{TOT}^{-1}\ dN/d\cos\theta$
2.0
1.5
1.0
.5
0
-1
0
1
$\cos\theta$

FIGURE 6

TECHNICAL INFORMATION DIVISION
LAWRENCE BERKELEY LABORATORY
UNIVERSITY OF CALIFORNIA
BERKELEY, CALIFORNIA 94720